EUROPEAN JOURNAL OF PURE AND APPLIED MATHEMATICS
2026, Vol. 19, Issue 1, Article Number 7369
ISSN 1307-5543 – ejpam.com
Published by New York Business Global

Dynamical Analysis on a Family of Sixth-Order Multiple-Zero Solver with Polynomial and Rational Weight Functions

Young Hee Geum

Department of Mathematics, Dankook University, Cheonan 330-714, Korea

Abstract. A sixth-order family of three-point multiple root solvers with polynomial and rational weight functions are investigated by means of Möbius conjugacy map applied to a prototype polynomial of the form $(z-p)^m(z-q)^m$ with the related parameter spaces and dynamical planes. The interesting dynamics is shown through various stability surfaces and parameter spaces including dynamical planes.

2020 Mathematics Subject Classifications: 65A05, 65D18

Key Words and Phrases: Conjugacy map, multiple root, nonlinear equation, parameter space

1. Introduction

Root-finding problems occupy a central position in numerical analysis[1–5] and scientific computing, serving as a cornerstone for the solution of a vast array of mathematical models. Fundamentally, these problems involve identifying the values of a variable x for which a prescribed function $f(x)$ attains zero[6]. A multiple root[6] of an equation $f(x)=0$ is a solution at which the function and several of its derivatives vanish. A value r is called a multiple root of multiplicity $m \geq 2$ if $f(r)=f'(r)=f''(r)=\cdots=f^{(m-1)}(r)=0,\ f^{(m)} \neq 0$. Their significance spans numerous disciplines—including artificial intelligence, engineering, economics, machine learning, and computational biology—where nonlinear equations frequently arise and analytic solutions are rarely obtainable. This pervasive complexity underscores the necessity for numerical schemes that are not only efficient and robust but also theoretically rigorous, enabling the accurate and stable approximation of roots in both classical and modern computational contexts.

Given their broad applicability and theoretical significance, root-finding problems[7–11] remain an active area of investigation[2, 12–17]. Advances in this domain not only enhance numerical performance but also deepen our understanding of the mathematical structures underlying complex systems.

DOI: https://doi.org/10.29020/nybg.ejpam.v19i1.7369

Email address: `conpana@empal.com` (Y. H. Geum)

Definition 1. *Let $f : X \to X$ and $g : Y \to Y$ be two functions. Two functions f and g are said to be conjugate if there is a function $h : X \to Y$ such that $h \circ f = g \circ h$. Then the map h is called a conjugacy. Two function F and G are said to be Möbius conjugate if there exists a Möbius transformation $M(z) = (z-A)/(z-B)$ with $A \neq B,\ A, B \in C \cup \{\infty\}$ such that*

$$G = M \circ F \circ M^{-1}.$$

This means that F and G are the same dynamical system up to a change of coordinates via a Möbius transformation.

A sixth-order family of three-point modified Newton-like multiple zero solvers is developed by Geum-Kim-Neta[18]. In this study, we have considered the form of mixture of polynomial and rational weight function below.

$$\begin{cases} y_n = x_n - m \cdot h(x_n),\ h(x_n) = \frac{f(x_n)}{f'(x_n)}, \\ w_n = x_n - m \cdot \Phi_f(u_1) \cdot h(x_n),\ u_1 = (f(y_n)/f(x_n))^{\frac{1}{m}}, \\ x_{n+1} = x_n - m \cdot \Psi_f(u_1, u_2) \cdot h(x_n),\ u_2 = (f(w_n)/f(x_n))^{\frac{1}{m}}, \end{cases} \tag{1}$$

where $\Phi : C \to C$ is a analytic function in a small neighborhood of the origin 0 and $\Psi_f : C^2 \to C$ is holomorphic in a small neighborhood of $(0, 0)$.

$$\begin{cases} \Phi_f(u_1) = 1 + u_1 + 2{u_1}^2, \\ \Psi_f(u_1, u_2) = \frac{1+u_1+2{u_1}^2+(a_0+a_1u_1)u_2}{1+(b_0+b_1u_1)u_2}, \end{cases} \tag{2}$$

where $a_0 = 1 + b_0,\ b_1 = -2 + a_1 - b_0$ and four parameters $a_0,\ a_1,\ b_0$ and b_1 define a linear system of rank 2. Therefore, any two of them can be solved in terms of remaining two free parameters. Here we select $b_0 = \lambda,\ a_1 = 0$ for brevity of analysis. $\Psi_f(u_1, u_2) = \frac{1+u_1+2{u_1}^2+(1+\lambda)u_2}{1+(\lambda+(-2-\lambda)u_1)u_2}$.

The numerical methods in (1) solving a nonlinear equation[2, 19, 20] is written as

$$x_{n+1} = R_f(x_n, \lambda, a_0, a_1, a_2),$$

where $R_f(x_n, \lambda, a_0, a_1, a_2) = x_n - m \cdot \Psi_f(u_1, u_2) \cdot h(x_n)$ is a fixed point operator.

The process of solving the nonlinear equation of $f(z) = 0$ is regarded as a sequence of images of initial value α_0 under $\mathtt{I}_f$ below:

$$\{\alpha_0, R_f(\alpha_0), {R_f}^2(\alpha_0), \cdots {R_f}^n(\alpha_0), \cdots\}$$

We investigate the conjugacy map and stability surfaces of the selected iterative scheme[13–15] in Section 2. The algorithm, the parameter spaces and the basins of attraction are shown in Section 3. Finally, conclusions are stated in the last section.

2. Conjugacy map and analysis

Via Möbius conjugacy map [3] $\mu(z) = (z-p)/(z-q)$ when applied to a polynomial $f(z) = ((z-p)(z-q))^m$, $\mathtt{I}_f$ is conjugated to $J(z,\lambda)$ with $z, p, q \in C\bigcup\{\infty\}$ and $p \neq q$ as follows

$$J(z,p,q,\lambda) = \frac{N(z,p,q,\lambda)}{D(z,p,q,\lambda)}, \tag{3}$$

where N and D are polynomials whose coefficients are dependent upon parameters p, q and λ.

With the aid of Mathematica [21], after the computation with $\mu^{-1}(z) = (qz-p)/(z-1)$, we obtain $J(z,\lambda)$ as follows

$$J(z,\lambda) = -z^4\frac{s_1 \cdot s_2}{s_3 \cdot s_4}, \tag{4}$$

where $s_1 = 5+4z+z^2$, $s_2 = 1+56z^5+28z^6+8z^7+z^8+z^2(28-9\lambda)-5z^4(-14+\lambda])-2z(-4+\lambda)-14z^3(-4+\lambda)$, $s_3 = 1+4z+5z^2$, $s_4 = 1+8z+28z^2+56z^3+z^8+z^6(28-9\lambda)-5z^4(-14+\lambda)-14z^5(-4+\lambda)-2z^7(-4+\lambda)$.

We find out that J is dependent only on λ but independent of parameter p and q. We find the fixed points of the iterative scheme $J(z,\lambda)$. Let $\phi(z,\lambda) = z - J(z,\lambda)$ where roots are the desired fixed points of $J(z,\lambda)$. After a lengthy computation, we find that $z=0$ and $z=1$ are the zeros of $\phi(z,\lambda)$ and the following expression of $\phi(z,\lambda)$:

$$\phi(z,\lambda) = z(1-z)\frac{P(z,\lambda)}{Q(z,\lambda)}, \tag{5}$$

where

$$\begin{aligned} P(z,\lambda) =& 1+13z+78z^2+281z^3+281z^9+78z^{10}+13z^{11}+z^{12}+z^4(671+5\lambda) \\ &+z^8(671+5\lambda)+z^5(1114+24\lambda)+z^7(1114+24\lambda)+z^6(1316+42\lambda), \\ Q(z,\lambda) =& (1+4z+5z^2)(1+8z+28z^2+56z^3+z^8+z^6(28-9\lambda)-5z^4(-14+\lambda) \\ &-14z^5(-4+\lambda)-2z^7(-4+\lambda)). \end{aligned}$$

Theorem 1. *Let $\phi(z,\lambda)$ be given by* (5). *Then the following hold.*
(1) If $\lambda = -\frac{4127}{4048}$, then

$$\phi(z,\lambda) = \frac{zP_1(z)}{Q_1(z)},$$

where $P_1(z) = 4048+48576z+263120z^2+821744z^3+1558085z^4+1714851z^5+743410z^6-743410z^7-1714851z^8-1558085z^9-821744z^{10}-263120z^{11}-48576z^{12}-4048z^{13}$, $Q_1(z) = (1+4z+5z^2)(4048+32384z+113344z^2+226688z^3+303995z^4+284466z^5+150487z^6+40638z^7+4048z^8)$.
(2) If $\lambda = -\frac{1408}{25}$, then

$$\phi(z,\lambda) = -(-1+z)^3 z\frac{P_2(z)}{Q_2(z)},$$

where $P_2(z) = 25 + 375z + 2675z^2 + 12000z^3 + 31060z^4 + 44178z^5 + 31060z^6 + 12000z^7 + 2675z^8 + 375z^9 + 25z^{10}$, $Q_2(z) = (1 + 4z + 5z^2)(25 + 200z + 700z^2 + 1400z^3 + 8790z^4 + 21112z^5 + 13372z^6 + 3016z^7 + 25z^8)$.

(3) If $\lambda = \frac{128}{15}$, *then*

$$\phi(z, \lambda) = \frac{zP_3(z)}{Q_3(z)},$$

where $P_3(z) = 15 + 195z + 1170z^2 + 4215z^3 + 10705z^4 + 19782z^5 + 25116z^6 + 19782z^7 + 10705z^8 + 4215z^9 + 1170z^{10} + 195z^{11} + 15z^{12}, Q_3(z) = (1 + 4z + 5z^2)(15 + 135z + 555z^2 + 1395z^3 + 1805z^4 + 853z^5 + 121z^6 - 15z^7)$.

(4) Let $\lambda \notin \{0, -\frac{4127}{4048}, -\frac{1408}{25}, \frac{128}{15}\}$. *Then* $P(z) = P(\frac{1}{z})z^{10}$.

Proof. (1)-(3) Suppose $P(z) = 0$ and $Q(z) = 0$ for z. Eliminating λ from the two polynomials, we have the relation $F = (1+z)(2+9z+16z^2+9z^3+2z^4) = 0$. Substituting all the roots of F into $P(z) = 0$ and $Q(z) = 0$, we get the relations for λ. Solving them for λ, we have $\lambda = 0, -\frac{4127}{4048}$. The remaining part is straightforward. If $(z - 1)$ is a divisor of $P(z)$, then we have $\lambda = -\frac{1408}{25}$. If $(z - 1)$ is a divisor of $Q(z)$, then we have $\lambda = \frac{128}{15}$. Then remaining proof is trivial. (4) By direct computation, we have $P(1/z) = z^{-10}P(z)$. □

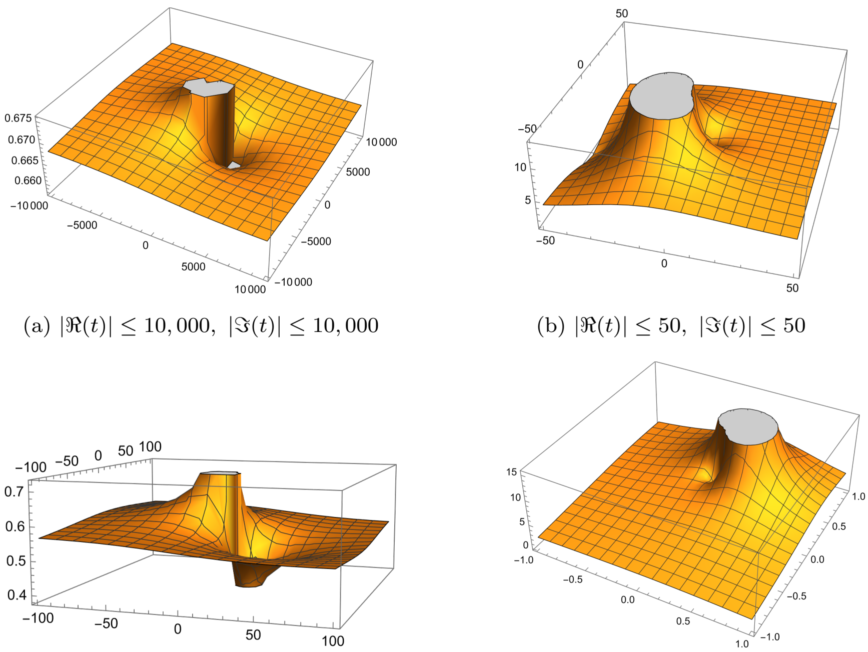

(a) $|\Re(t)| \le 10,000,\ |\Im(t)| \le 10,000$ (b) $|\Re(t)| \le 50,\ |\Im(t)| \le 50$

(c) $|\Re(t)| \le 100,\ |\Im(t)| \le 100$ (d) $|\Re(t)| \le 1,\ |\Im(t)| \le 1$

Figure 1: Stability surfaces .

To find the stability of fixed points, we compute the derivative of $J(z, \lambda)$ as follows:

$$J'(z, \lambda) = 2z^3 \frac{R(z, \lambda)}{W(z, \lambda)^2}, \tag{6}$$

where

$$\begin{aligned} R(z, \lambda) =& 10 + s_1 z + s_2 z^2 + s_3 z^3 + s_4 z^4 + s_5 z^5 + s_6 z^6 + s_7 z^7 + s_8 z^8 + s_9 z^9 \\ &+ s_{10} z^{10} + s_9 z^{11} + s_8 z^{12} + s_7 z^{13} + s_6 z^{14} + s_5 z^{15} + s_4 z^{16} + s_3 z^{17} \\ &+ s_2 z^{18} + s_1 z^{19} + 10 z^{20},\ W(z, \lambda) = t_3 t_4, \\ s_1 =& -25(-8 + \lambda),\ s_2 = 1900 - 399\lambda,\ s_3 = -3(-3800 + 981\lambda), \\ s_4 =& -6(-8075 + 2203\lambda),\ s_5 = 155040 - 40214\lambda + 25\lambda^2, \\ s_6 =& 387600 - 87552\lambda + 265\lambda^2,\ s_7 = 775200 - 141578\lambda + 1261\lambda^2, \\ s_8 =& 2(629850 - 88751\lambda + 1746\lambda^2),\ s_9 = 2(839800 - 93220\lambda + 3109\lambda^2), \\ s_{10} =& 2(923780 - 92529\lambda + 3739\lambda^2),\ s_{11} = 2(839800 - 93220\lambda + 3109\lambda^2). \end{aligned}$$

Theorem 2. *Let $J'(z, \lambda)$ be given by (6). Then the following hold.*

(1) If $\lambda = -\frac{128}{15}$, then

$$J'(z, \lambda) = \frac{-4z^3 R_1(z)}{{W_1}^2},$$

where $R_1(z, \lambda) = 1125 + 750z - 168915z^2 - 1881360z^3 - 10832460z^4 - 40742200z^5 - 108925980z^6 - 215484528z^7 - 322122282z^8 - 367849580z^9 - 322122282z^{10} - 215484528z^{11} - 108925980z^{12} - 40742200z^{13} - 10832460z^{14} - 1881360z^{15} - 168915z^{16} + 750z^{17} + 1125z^{18}$, $W_1(z, \lambda) = (1 + 4z + 5z^2)(15 + 135z + 555z^2 + 1395z^3 + 1805z^4 + 853z^5 + 121z^6 - 15z^7)$.

(2) If $\lambda = \frac{1024}{25}$, then

$$J'(z, \lambda) = 4(-1 + z)^2 z^3 \frac{R_2(z, \lambda)}{W_2(z, \lambda)^2},$$

where $R_2(z) = 3125 - 251250z - 5019075z^2 - 43894800z^3 - 236820300z^4 - 882927800z^5 - 2389639580z^6 - 4805172592z^7 - 7268261258z^8 - 8332884140z^9 - 7268261258z^{10} - 4805172592z^{11} - 2389639580z^{12} - 882927800z^{13} - 236820300z^{14} - 43894800z^{15} - 5019075z^{16} - 251250z^{17} + 3125z^{18}$,
$W_2(z) = (1 + 4z + 5z^2)(25 + 200z + 700z^2 + 1400z^3 - 3370z^4 - 12936z^5 - 8516z^6 - 1848z^7 + 25z^8)$.

(3) If $\lambda = \frac{864}{125}$, then

$$J'(z, \lambda) = 4z^3 \frac{R_3(z, \lambda)}{W_3(z, \lambda)^2},$$

where $R_3(z) = 78125 + 212500z - 6702250z^2 - 69859500z^3 - 335256375z^4 - 950974800z^5 - 1600772280z^6 - 1118296272z^7 + 1559680266z^8 + 5374971064z^9 + 7232079044z^{10} + 5374971064z^{11} + 1559680266z^{12} - 1118296272z^{13} - 1600772280z^{14} - 950974800z^{15} - 335256375z^{16} - 69859500z^{17} - 6702250z^{18} + 212500z^{19} + 78125z^{20}$,
$W_3(z) = (1+4z+5z^2)(125+1000z+3500z^2+7000z^3+4430z^4-5096z^5-4276z^6-728z^7+125z^8)$.

(4) Let $\lambda \notin \{-\frac{128}{15}, \frac{1024}{25}, \frac{864}{125}\}$. *Then* $R(z) = z^{20}R(\frac{1}{z})$

Proof. (1)-(3) Suppose that $R(z) = 0, W(z) = 0$ for z. By eliminating λ from $R(z) = 0$, and $W(z) = 0$, we get the relation $T(z)$. Substituting all the roots of $T(z)$ into $R(z) = 0$ and $W(z) = 0$, we find $\lambda = -\frac{128}{15}, \frac{1024}{25}, \frac{864}{125}$. □

The stability surfaces are shown by illustrative conical surfaces in Figure 1.

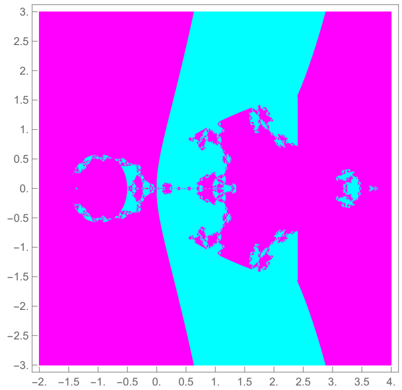

(a) $\lambda = -128/15$

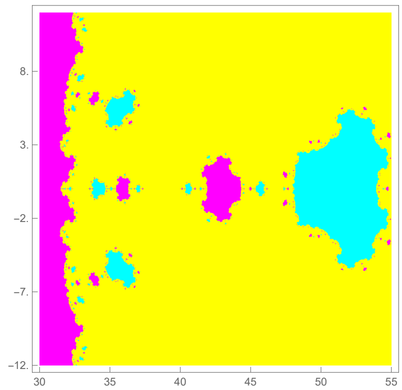

(b) $\lambda = -7$

Figure 2: Parameter spaces.

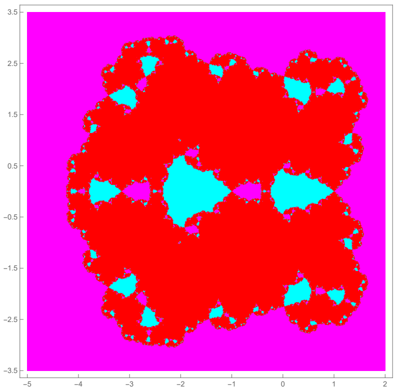

(a) $\lambda = -128/15$

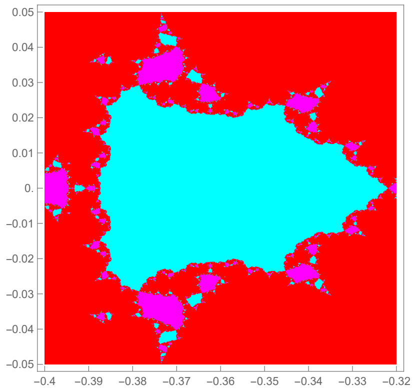

(b) $\lambda = -7$

Figure 3: Basins of attraction associated with J.

3. Experiment

According to Algorithm 1, the numerical parameter spaces[22–24] are constructed in Figure 2. The systematic color palette in Table 1 is utilized to paint a value according to the orbital period of the point z of $J(z, \lambda)$. The tolerance of 10^{-4} after up to 400 iterations is assigned using Mathematica[21].

Algorithm 1

(1) Set $i = 1$
(2) Select a region $B \in C$ and choose a point $v = (Re(v), Im(v))$ in B
(3) For the v, compute the free critical point.
(4) Find out the orbit of $J(z, t)$ within the maximal iterative number.
(5) If the orbit converges to one cycle within the error, then color the point v according to the color palette in Table 1.
(6) Choose the next value in B
(7) Repeat steps (2)-(6) until desired result is obtained.
(8) Set $i = i + 1$ and if $i \leq w$, then repeat steps (2)-(8)

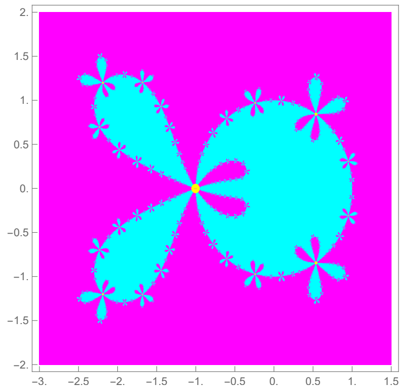

(a) $\lambda = 0$

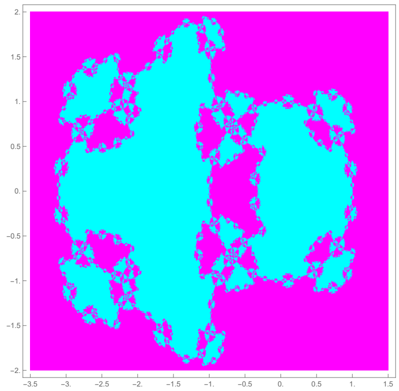

(b) $\lambda = 1$

Figure 4: Basins of attraction associated with J.

(9) If $i = w$, then stop the process.

Let $\mathcal{P} = \{\lambda \in C :$ a critical orbit of z converges to a number $w_p \in \overline{\mathbb{C}}\}$. It is called the parameter space. There are finite periods in the orbit if the number w_p is a finite constant. Otherwise, the orbit is not periodic however it is bounded or goes to infinity. Let $\mathcal{D} = \{z \in C :$ an orbit of z under J converges to a number $w_d \in \overline{\mathbb{C}}\}$, which is called the dynamical plane associated with $J(z, \lambda)$.

Theorem 3. *Let $z(\lambda)$ be a free critical point of $J(z, \lambda)$. Then the parameter space is symmetric with respect to its horizontal axis.*

Proof. Let $z(\lambda)$ is a root of $P(z, \lambda)$. Then $\bar{z}(\bar{\lambda})$ is a root of $P(z, \lambda)$ at $\bar{\lambda}$. From conjugated map $J(z, \lambda)$, we obtain

$$\begin{aligned}|J(z,\lambda)| =& |J(z(\lambda),\lambda)| = |\overline{J(z(\lambda),\lambda)}| \\ =& |J(\overline{z(\lambda)},\bar{\lambda})| = |J(\bar{z}(\bar{\lambda}),\bar{\lambda})|.\end{aligned}$$

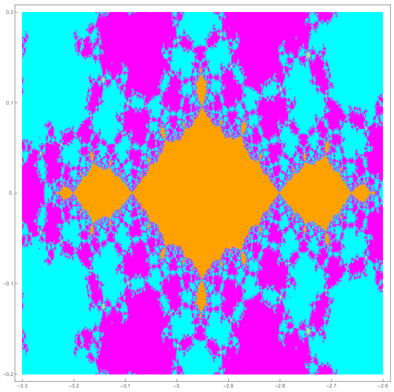

(b) $\lambda = 7$

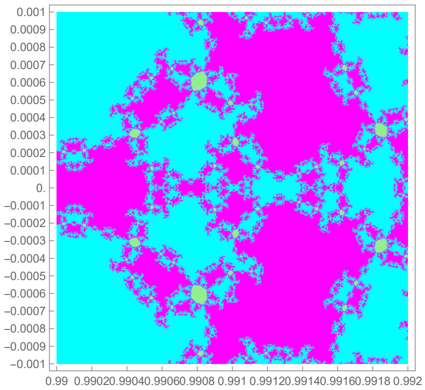

(a) $\lambda = 128/15$

Figure 5: Basins of attraction associated with J.

Then the parameter space with $J(z, \lambda)$ is symmetric with respect to its horizontal axis. □

The parameter spaces $\mathcal{P}$ are illustrated in Figure 2. A point $\epsilon \in \mathcal{P}$ is painted using the color palette in Table 1. A point is painted in cyan if the iteration of the method starting in z_0 converges to the fixed point 0, in magenta if it converges to ∞ and in yellow if the iteration converges to 1.

In Figures 3-5 appear the basins of attraction with the selected values. It is clear that there exist members of the family with complicated behavior. In Figure 5, the dynamical plane of a member of the family with regions of convergence to an attracting 2-cycle and an attracting 3-cycle are shown.

We paint the initial points on the basins of attraction with various colors ranging from bright ones to dark ones according to the iteration number for convergence. In Figure 3-5, the black points mean the points for which the corresponding iteration method starting from an initial point do not converge to any roots of the selected test function.

The typical cases of methods Y_k in methods (2) are used for $1 \leq k \leq 6$ with selected

Table 1: Color palette for a n-periodic orbit with $n \in N \cup \{0\}$

n	C_n
$n = 1$	$C_1 = \begin{cases} \text{magenta, for fixed point } \infty \\ \text{cyan, for fixed point } 0 \\ \text{yellow, for fixed point } 1 \\ \text{red, for other strange fixed point ,} \end{cases}$
$2 \leq n \leq 68$	C_2 = orange, C_3 = light green, C_4 = dark red, C_5 = dark blue, C_6 = dark green, C_7 = dark yellow, C_8 = floral white, C_9 = light pink, C_{10} = khaki, C_{11} = dark orange, C_{12} = turquoise, C_{13} = lavender, C_{14} = thistle, C_{15} = plum, C_{16} = orchid, C_{17} = medium orchid, C_{18} = blue violet, C_{19} = dark orchid, C_{20} = purple, C_{21} = power blue, C_{22} = sky blue, C_{23} = deep sky blue, C_{24} = dodger blue, C_{25} = royal blue, C_{26} = medium spring green, C_{27} = spring green, C_{28} = medium sea green, C_{29} = sea green, C_{30} = forest green, C_{31} = olive drab, C_{32} = bisque, C_{33} = moccasin, C_{34} = light salmon, C_{35} = salmon, C_{36} = light coral, C_{37} = Indian red, C_{38} = brown, C_{39} = fire brick, C_{40} = peach puff, C_{41} = wheat, C_{42} = sandy brown, C_{43} = tomato, C_{44} = orange red, C_{45} = chocolate, C_{46} = pink, C_{47} = pale violet red, C_{48} = deep pink, C_{49} = violet red, C_{50} = gainsboro, C_{51} = light gray, C_{52} = dark gray, C_{53} = gray, C_{54} = charteruse, C_{55} = electric indigo, C_{56} = electric lime, C_{57} = lime, C_{58} = silver, C_{59} = teal, C_{60} = pale turquoise, C_{61} = sandy brown, C_{62} = honeydew, C_{63} = misty rose, C_{64} = lemon chiffon, C_{65} = lavender blush, C_{66} = gold, C_{67} = crimson, C_{68} = tan.
$n = 0^*$ or $n > 69$	C_n = black.

$*$: $n = 0$: the orbit is non-periodic but bounded.

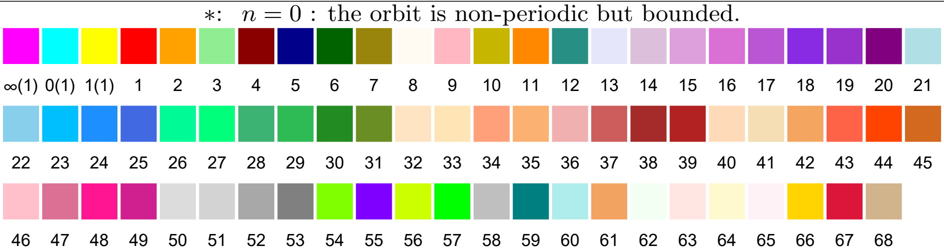

parameters $\lambda = -1, -0.2, -0.1, 0.1, 0.5, 1$, respectively. The following sixth-order multiple-root finders developed by Geum [16] are conveniently denoted by M_1, M_2, M_3 for later use.

$$\begin{cases} y_n = x_n - m\frac{f(x_n)}{f'(x_n)}, \\ w_n = x_n - mA_f(k)\frac{f(x_n)}{f'(x_n)}, \ \ k = (\frac{f'(y_n)}{f'(x_n)})^{\frac{1}{m-1}}, \\ x_n = x_n - mB_f(k,v)\frac{f(x_n)}{f'(x_n)}, \ \ v = (\frac{f(w_n)}{f(x_n)})^{\frac{1}{m}}, \end{cases} \tag{7}$$

where $A_f : C \to C$ is analytic in a small neighborhood of 0 and $B_f : C^2 \to C$ is holomorphic in a neighborhood of $(0, 0)$.

$$\begin{aligned} M_1 : A_f(k) =& 1 + k + \frac{2m}{-1+m}k^2, \ \ B_k(k,v) = 1 + k + \frac{2m}{-1+m}k^2 + (1+2k)v \\ M_2 : A_f(k) =& 1 + k + \frac{2m}{-1+m}k^2, \ \ B_k(k,v) = 1 + k + \frac{2m}{-1+m}k^2 + (1+2k+k^2)v \\ M_3 : A_f(k) =& 1 + k + \frac{2m}{-1+m}k^2, \ \ B_k(k,v) = 1 + k + \frac{2m}{-1+m} + k^5 + (1+2k)v. \end{aligned}$$

Table 2: $p_1(z) = (7z^2 + 1)^2$

method	cpu	tcon	avg	tdiv
Y_1	562.812	360,000	17.0847	0
Y_2	107.391	360,000	4.25112	0
Y_3	118.625	360,000	4.32727	0
Y_4	640.203	360,000	14.2556	0
Y_5	872.656	360,000	14.1185	0
Y_6	521.438	360,000	14.137	0
M_1	173.36	359,850	10.4043	150
M_2	286.875	359,644	10.7436	356
M_3	175.297	359,862	10.4028	138

Table 3: $p_2(z) = (z^2 + z + 7)^3$

method	cpu	tcon	avg	tdiv
Y_1	3151.13	360,000	13.2533	0
Y_2	2213.11	360,000	10.195	0
Y_3	2174.41	360,000	9.83093	0
Y_4	1688.98	360,000	8.06614	0
Y_5	1691.01	360,000	7.99121	0
Y_6	1717.24	360,000	8.02049	0
M_1	479.453	359,910	10.0726	90
M_2	453.438	359,990	9.44209	10
M_3	376.61	359,993	9.47263	7

As a first example, we have taken the following polynomial

$$p_1(z) = (7z^2 + 1)^2$$

whose roots are $\alpha = \pm 0.3771i$ of multiplicity 2. The statistical results are listed in Table 2 and relevant basins of attraction are shown in Figure 6. In Table 2, abbreviations **cpu, tcon, avg** and **tdiv** denote CPU time measured in units of seconds for convergence, the number of total convergent points, the number of average iteration for convergence and the number of divergent points, respectively. The method Y_2 has shown best **avg** and **tdiv**. As can be seen in Figure 6, methods M_1, M_2 and M_3 have shown considerable amount of black points.

As a second example, we have taken the following polynomial whose roots are all of multiplicity three

$$p_2(z) = (z^2 + z + 7)^3$$

whose roots are $z = -0.5 \pm 2.59808i$. The statistical results are shown in Table 3 and related basin of attraction are illustrated in Figure 7. The method $Y5$ has shown best **avg**.

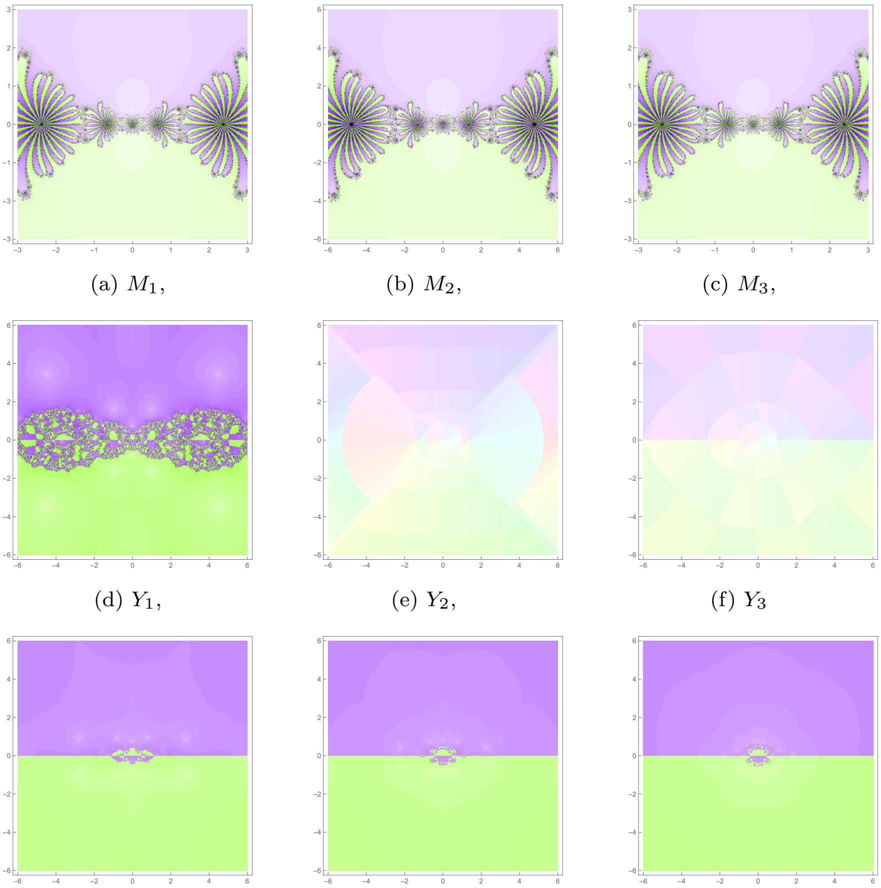

(a) M_1, (b) M_2, (c) M_3,

(d) Y_1, (e) Y_2, (f) Y_3

(g) Y_4, (h) Y_5, (i) Y_6

Figure 6: Basins of attraction for $p_1(z) = (7z^2 + 1)^2$.

4. Conclusion

We have investigated a class of sixth-order multiple-root finder with polynomial and rational weight functions via Möbius conjugacy map applied to polynomial of the form $f(z) = (z - p)^m (z - q)^m$ and considered the complex dynamical analysis on the Riemann sphere by drawing the parameter spaces associated with the free critical points and the basins of attraction to solve the nonlinear equations. A future analysis handling with the dynamics of other types of iterative methods will be considered to construct favorable parameter spaces and dynamical planes. To get information on better initial values of an numerical method, we need to investigate the basins of attraction. We have illustrated the basins of attraction as well as statistical analysis featuring date for CPU time and other tabulated numbers for convergence behavior. As a future work, we will develop a higher-order class of methods along with statistical date analysis as well as an illustrative investigation of the desired dynamical behavior.

Conflicts of Interest : The author declare no conflict of interest.

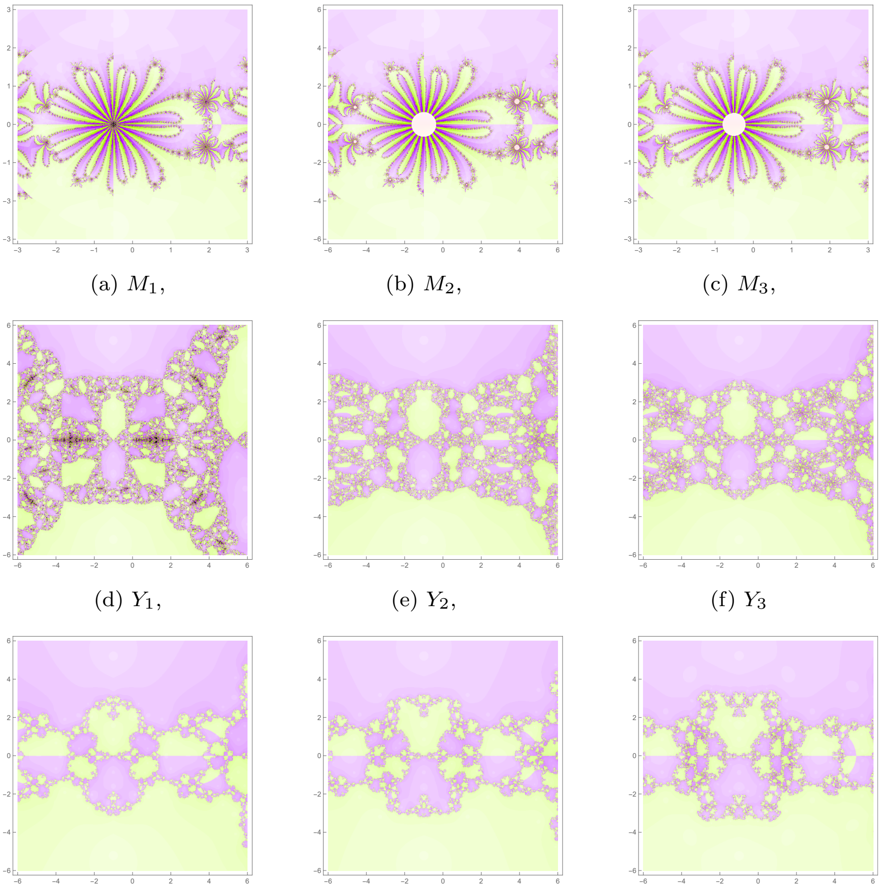

(a) M_1, (b) M_2, (c) M_3,

(d) Y_1, (e) Y_2, (f) Y_3

(g) Y_4, (h) Y_5, (i) Y_6

Figure 7: Basins of attraction for $p_2(z) = (z^2 + z + 7)^3$.

References

[1] L. V. Ahlfors. *Complex Analysis*. McGraw-Hill Book Inc., 1979.

[2] S. Amat, S. Busquier, and S. Plaza. Review of some iterative root-finding methods from a dynamical point of view. *Scientia*, 10:3–35, 2004.

[3] P. Blanchard. The dynamics of newton's method. *Proceedings of Symposia in Applied Mathematics*, 49:139–154, 1994.

[4] R. L. Burden, J. Faires, and A. Reynolds. *Numerical Analysis*. PWS Publishers, 1981.

[5] J. F. Traub. *Iterative Methods for the Solution of Equations*. Chelsea Publishing Company, 1982.

[6] H. T. Kung and J. F. Traub. Optimal order of one-point and multipoint iteration. *Journal of the ACM*, 21:643–651, 1974.

[7] R. L. Devaney. Complex dynamical systems: The mathematics behind the mandelbrot and julia sets. *Proceedings of Symposia in Applied Mathematics*, 49:1–29, 1994.

[8] L. Hörmander. *Introduction to Complex Analysis in Several Variables*. North-Holland Publishing Company, 1973.

[9] S. Lipschutz. *Theory and Problems of General Topology*. McGraw-Hill Inc., 1965. Schaum's Outline Series.

[10] H. Peitgen and P. Richter. *The Beauty of Fractals*. Springer-Verlag, 1986.

[11] B. V. Shabat. *Introduction to Complex Analysis, Part 2: Functions of Several Variables*. American Mathematical Society, 1992.

[12] Y. H. Geum and Y. I. Kim. A cubic-order variant of newton's method for finding multiple roots of nonlinear equations. *Computers & Mathematics with Applications*, 62:1634–1640, 2011.

[13] F. Chicharro, A. Cordero, J. Gutiérrez, and J. Torregrosa. Complex dynamics of derivative-free methods for nonlinear equations. *Applied Mathematics and Computation*, 219:7023–7035, 2013.

[14] C. Chun and B. Neta. Basins of attraction for zhou–chen–song fourth order family of methods for multiple roots. *Mathematics and Computers in Simulation*, 109:74–91, 2015.

[15] A. Cordero, J. García-Maimó, J. R. Torregrosa, M. P. Vassileva, and P. Vindel. Chaos in king's iterative family. *Applied Mathematics Letters*, 119:842–848, 2016.

[16] Y. H. Geum. On constructing a family of sixth-order methods for multiple roots. *Fractal and Fractional*, 7:878–892, 2023.

[17] Á. A. Magréñan, A. Cordero, J. M. Gutiérrez, and J. R. Torregrosa. Real qualitative behavior of a fourth-order family of iterative methods by using the convergence plane. *Mathematics and Computers in Simulation*, 105:49–61, 2014.

[18] Y. H. Geum, Y. I. Kim, and B. Neta. A sixth-order family of three-point modified newton-like multiple-root finders and their dynamics behind their extraneous fixed points. *Applied Mathematics and Computation*, 283:120–140, 2016.

[19] A. F. Beardon. *Iteration of Rational Functions*. Springer-Verlag, New York, 1991.

[20] R. Behl, A. Cordero, S. Motsa, and J. Torregrosa. On developing fourth-order optimal families of methods for multiple roots and their dynamics. *Applied Mathematics and Computation*, 265:520–532, 2015.

[21] S. Wolfram. *The Mathematica Book*. Wolfram Media, 5 edition, 2003.

[22] Y. H. Geum. On a sixth-order solver for multiple roots of nonlinear equations. *European Journal of Pure and Applied Mathematics*, 17:710–720, 2024.

[23] Y. H. Geum. On dynamics of a sixth-order multiple-root finder for nonlinear equations. *Journal of Applied Mathematics and Informatics*, 42:213–221, 2024.

[24] D. Gulick. *Encounters with Chaos*. McGraw-Hill Inc., 1992.